EVOLUTION OF NEUTRAL-BEAM-DRIVEN CURRENT IN TOKAMAK PLASMAS
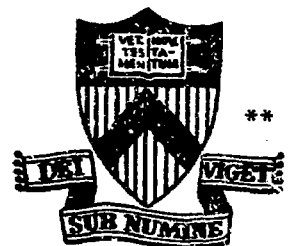
BY

C. E. SINGER, L. BROMBERG,
J. HOVEY, AND D. L. JASSBY

PLASMA PHYSICS LABORATORY

MASTER

PRINCETON   UNIVERSITY
PRINCETON, NEW JERSEY

PPL- 45

EVOLUTION OF NEUTRAL-BEAM-DRIVEN CURRENT IN TOKAMAK PLASMAS

C. E. Singer, L. Bromberg, J. Hovey, D. L. Jassby

Princeton Plasma Physics Laboratory, Princeton, NJ 08540   U.S.A.

ABSTRACT. Neutral-beam heating and current induction have been analyzed with a one-dimensional model that includes a Fokker-Planck analysis of the circulating ion current, the time and space dependence of the electron 'return' current, and the steady electron shielding current including electron trapping effects. With 1.2 MW of 40 keV H^0 injected tangentially into a 25-cm radius PLT plasma with $\langle n_e \rangle = 2.0 \times 10^{13}$ cm^{-3}, the maximum beam-driven current is about 100 kA and results in a 0.24-V reduction in loop voltage. Reversed loop voltages should be observable in low density plasmas in ISX-B and TFTR, which would provide an unambiguous detection of the beam-driven current. When the radial profiles of beam-driven current are less peaked than the ohmic-current profile, the profiles of the 'safety factor' q should be more stable to n=1, m=1 and n=1, m=2 kink modes, if the total plasma current is kept constant.

1. INTRODUCTION

The maintenance of a steady-state tokamak current by continuous neutral-beam injection [1,2] is problematical for a large dense plasma because of the difficulty of beam penetration. Establishment of a beam-driven current is more feasible at the early stages of start-up, where the plasma opacity is necessarily small, and when intense heating is required in any event. Both the resistive and inductive flux swings that must be supplied by the central ohmic-heating transformer can be reduced significantly by initiating neutral-beam injection parallel to the plasma current, I_p, when I_p is just large enough to confine co-injected ions (i.e., $I_p \sim 200$ to 300 kA). The electron temperature is rapidly raised to the 2-keV range, so that further requirements for 'resistive flux swing' are minimal. A large plasma current can be driven by the circulating fast ions, and by the flux swing that results as the equilibrium vertical field is increased to accommodate the increasing current and plasma pressure [3]. Present large beam-injected tokamak plasmas have a size, current, and temperature comparable with those expected for the initial 2-MA phase of reactor-sized tokamaks.

Previous analyses [1,2,4,5] have treated the beam-driven current only in steady-state, and with no radial dependences. In the present work, neutral-beam heating and current induction are analyzed with a one-dimensional model, described in Section 2, which includes a Fokker-Planck analysis of the circulating ion current, the time and space dependences of the transient electron return current, and the steady electron shielding current. This model is used in Section 3 to find the general conditions under which the beam-driven current can be maximized. In Section 4, the theoretical model is applied to several contemporary tokamaks. The reduction in loop voltage produced by the beam-driven current is found to be the most directly useful machine parameter for detecting beam-driven currents, and is also the principal parameter of interest in start-up scenarios for large tokamaks and in steady-state operation. Section 5 examines the stability of the plasma current profile when the beam-driven current is relatively strong.

2. COMPUTATIONAL MODEL

Calculation of the beam-driven current requires consideration of the following physical processes.

(1) The particle and energy balances of the background plasma.

(2) The injection profile, slowing down, and pitch-angle scattering of the fast ions.

(3) A reduction of the circulating ion current, I_{circ}, by a shielding current, I_s, produced by electrons accelerated by momentum transfer from the circulating fast ions. This collisional shielding current forms very rapidly and persists in the steady state [1-4]. The sum of I_{circ} and I_s will be referred to as the net beam-driven current, I_{bd}.

(4) The electromagnetic induction of a 'return' current, I_{ret}, as the net beam-driven current is turned on, and the subsequent resistive decay of I_{ret}. The sum of I_{bd} and I_{ret} will be denoted by I'_{bd}.

Table 1 lists the notation used for the various plasma currents in the presence of neutral beam injection.

2.1 Background Plasma

The calculation of ion and electron energy balances includes beam and ohmic heating, electron-ion collisions, and radiative and transport losses. The radiative and transport losses are combined and described by the empirically determined electron and ion energy loss times, $\tau_{Ee} = 5 \times 10^{19} <n_e> a_p^2$, which is slightly modified from Ref. [6], and $\tau_{Ej} = 7 \times 10^{-5} a_p^2$

Table 1. Notation for Currents
I_{circ}=Circulating ion current
I_s =Collisional electron shielding
I_{ret} =Electron return current
I'_{bd} =$I_{circ} + I_s + I_{ret}$
I_{bd} =$I_{circ} + I_s$
I_{OH} =Ohmic heating current
I_{tot} =$I'_{bd} + I_{OH}$

[7,8]. Here a_p is the minor radius, $<n_e>$ is the volume-averaged density, and cgs units are used.

For the calculations herein, $<n_e>$ is taken to be constant. A detailed consideration of particle balance including empirical transport loss, beam fueling, recycling, and gas puffing, shows that a constant density can be maintained provided that (a) the particle loss time $\tau_p \leqslant 3\tau_{Ee}$, (b) the wall recycling coefficient does not exceed 70%, and (c) a large flux of cold neutral gas is not introduced from the beam lines.

The energy and particle balance models determine the volume-averaged quantities $<T_e>$, $<T_i>$, and $<n_e>$. While arbitrary profiles of plasma parameters can be used, in this paper we report the results for parabolic density profiles and parabolic-squared temperature profiles, as these correspond well to profiles from experimental measurements and detailed transport-code computations [9].

2.2 Circulating Ion Current

The calculation of the circulating ion current starts from the drift-kinetic equation [5] for the fast-ion distribution function, $\bar{f}_h(\bar{v})$. We include charge-exchange loss but neglect electric-field acceleration and energy diffusion caused by the bulk-plasma thermal distribution. Dimensional analysis shows these corrections to be of the order of 10% or less for the cases reported herein. We also neglect self-interaction of the beam ions, because these collisions conserve momentum and therefore produce no direct effect on the current.

We find the circulating ion current by solving directly for the first angular moment of $f_h(\bar{v})$, that is, for

$$F_\zeta = 2\pi \int_{-1}^{1} f_h(\vec{v}) \; \zeta \; d\zeta \qquad (1)$$

where ζ is cosine of the pitch angle measured from the toroidal direction. The drift-kinetic equation is integrated and solved by a multigroup method [10] to find the circulating ion current density. The fast-ion source function S_ζ is determined by the neutral-beam trapping profile, which is computed by the FREYA neutral-beam deposition code [11]. In the present examples, the neutral-beam trapping profile is peaked at the plasma center, and is found to decrease nearly linearly with plasma radius.

2.3 Electron Shielding Current

The beam-driven current density is

$$J_{bd} = e\left(\int_{0}^{v_b} v^3 \; F_\zeta dv\right)\left[1 - \frac{1}{Z_{eff}} + \frac{1.46 \; A(Z_{eff})}{Z_{eff}} \left(\frac{r}{R}\right)^{1/2}\right] \qquad (2)$$

where $A(Z_{eff}) \approx 1 + 0.7/Z_{eff}$ [4], $v_b = (2E_b/M_b)^{1/2}$, and E_b is the beam energy. The second term on the right side is due to the streaming of electrons caused by collisional momentum transfer from the circulating ions (the 'shielding current'), and the third term is the reduction of this effect by the trapping of electrons in banana orbits.

2.4 Decay of Return Current

The build-up of the net beam-driven current I_{bd} induces a plasma return current. The total current $I_r(r)$ inside a circle of minor radius r is found from

$$\frac{\partial I_r}{\partial t} = \frac{rc^2}{2} \frac{\partial E}{\partial r} \qquad (3)$$

and

$$E = \frac{1}{\sigma}\left[\frac{1}{2\pi r} \; \frac{\partial I_r}{\partial r} - J_{bd}\right] \qquad (4)$$

where σ is the neoclassical conductivity. We compute the evolution of the voltage V_{loop} at the plasma boundary as a function of time after the start of beam injection, subject to the boundary condition of constant total plasma current, I_{tot}. The effect of the beam-driven current is to produce a loop voltage drop due to the J_{bd} term in Eq. (4).

We have also calculated the total plasma current subject to the boundary condition of constant loop voltage. In this case the transient beam-driven current I_{bd}' is added to the ohmic heating current, I_{OH}, so that the total current approaches the value $(I_{OH} + I_{bd})$ on the timescale of the plasma skin current. The results given in this paper, however, are computed only with the constant-current boundary condition, because this condition is the most appropriate for practical tokamak operation.

3. MAXIMIZING THE BEAM-DRIVEN CURRENT

The conditions for maximizing I_{bd} are found from the need to maximize the circulating ion current and to minimize the collisional electron shielding current. The circulating ion current is inversely proportional to $<n_e>$, increases with $<T_e>$, and decreases with Z_{eff} because of pitch-angle scattering; the shielding current decreases with Z_{eff}. Thus I_{bd} can be maximized when $<n_e>$ is small, $<T_e>$ is large, and $Z_{eff} \sim 2$. With

$Z_{eff} < 3$ and $T_e < 0.1 \, E_b$ (so that electron drag is dominant), one can show that the beam-driven current density is

$$J_{bd} \propto S_\zeta \, \frac{T_e^{3/2}}{n_e} \, (1 - \frac{1}{Z_{eff}}) \qquad (5)$$

4. PREDICTIONS FOR CONTEMPORARY TOKAMAKS

We have analyzed 3 near-term injection experiments, for which the parameters are listed in Table 2. Beam-injection experiments to date have

Table 2. <u>Machine Parameters</u>

	PLT	ISX-B	TFTR
Major radius (cm)	132	92	250
Minor radius (cm)	25	25	60
Magnetic field (T)	3.3	1.8	5.2
I_{OH} at $q_a = 3$ (MA)	0.26	0.20	1.12
Background species	D	D	D
Neutral Beams			
Species	H°	H°	D°
Energy (keV)	40	40	120
Power at full energy (MW)	1.2	2.4	15
Pulse length (s)	0.2	0.3	1.0
Tangency radius (cm)	112	74	211
Z_{eff}	2	2	2
$<T_e>$, ohmic (keV)	0.5	0.4	0.9
$<T_e>$, beam (keV)	0.9	1.7	3.3

used only moderate injected powers and pulse lengths, and there has been no attempt to optimize $<n_e>$ or Z_{eff}. For example, the I_{bd} predicted from our model for the low-density PLT experiments performed in 1977 with a 500-kW, 38-keV H° beam [12] is 30 kA, which is less than 10% of the ohmic current. At the end of the 0.1-s pulse, I'_{bd} is less than 10 kA.

4.1 Loop Voltage

Figure 1 shows the loop voltage computed for high power PLT beam injection with and without the beam-driven current, with the total current kept constant so that $q(a_p)=3.0$. Without the beam-driven current, the loop voltage drops because of electron heating. The much larger drop that occurs with the beam-driven current, just after the beam is turned, is the back emf induced by that portion of the beam deposited near the plasma edge, where J_{ret} decays rapidly. This transient back-emf signature of the beam-driven current is more apparent in Fig. 2, which shows the difference between the loop voltage calculated with and without the beam-driven current. This volt-
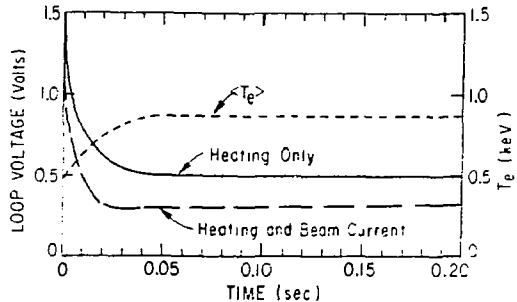

Fig. 1. Loop voltage and spatially-averaged T_e in PLT with neutral beam co-injection, with and without the beam-driven current. Injection begins at $t = 0$. $<n_e> = 3.5 \times 10^{13}$ cm^{-3}.

age difference ΔV is the 'transformer savings' provided by I_{bd}. The transient back-emf decays on the skin time scale, which is of the order of 100 ms for PLT and ISX-B. Table 3 shows the loop voltage at the end of the beam pulse, compared with the voltage calculated with the same plasma heating, but with no beam-driven current. Note that for ISX-B and TFTR, the transformer flux must be reversed to maintain constant total current, if the beam-driven current is included. In a longer pulse, the loop voltage would approach the value needed to drive the residual steady state ohmic current, that is $I_{OH} = I_{tot} - I_{bd}$.

Thus if the beam power is sufficiently large, I_{OH} can be completely replaced by I_{bd}, and the loop voltage rapidly goes to zero, or even changes sign. This result would provide the most convincing experimental demonstration of the beam-driven current, and zero loop voltage is also necessary for operating a steady-state tokamak.

Fig. 2. Change in loop voltage due to beam-driven current. $\langle n_e \rangle = 2 \times 10^{13}$ cm^{-3} (solid lines) and 3.5×10^{13} cm^{-3} (dashed lines). Injection begins at $t = 0$.

Plasma Rotation. In all the experiments analyzed here, the momentum input from the beams is easily large enough to raise the bulk-ion thermal velocity above the sonic velocity, in the absence of any drag. This rotation will produce current density that adds to the beam-driven current, and is shown in Table 3 for the case of rotation at the sonic speed. If rotation is undesirable, it can be damped by a toroidal-field ripple of the order of 1% or less [4]. In large devices such as TFTR where the beam-driven current may find use chiefly during start-up, the plasma can be located at relatively large major radius where the ripple strength exceeds 1%.
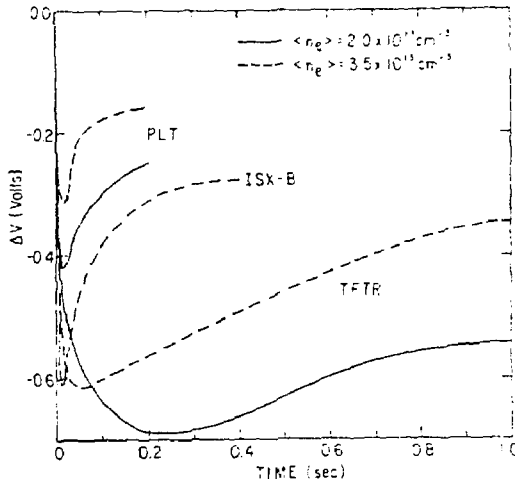
Table 3. Loop Voltages, Beam-Driven Currents, and Rotation

	PLT		ISX-B		TFTR	
$\langle n_e \rangle$ (10^{13} cm^{-3})	2.0	3.5	2.0	3.5	2.0	3.5
V_{loop}(Heating + beam)*	0.26	0.33	-0.27	-0.16	-0.43	-0.26
V_{loop}(Heating only)*	0.50	0.50	0.10	0.10	0.10	0.09
I_{bd} (MA)	0.12	0.07	0.56	0.38	3.02	1.90
I_{sonic} (MA)	0.16	0.21	0.41	0.53	3.38	4.54

*At end of beam pulse.

5. STABILITY OF CURRENT PROFILES

The effect of the beam-driven current on the stability of the current profile depends on whether $J_{bd}(r)$ is more or less peaked than $J_{OH}(r)$. For the case of constant plasma current, Fig. 3 illustrates the effects of a relatively flat $J_{bd}(r)$. The increased current at $r > 15$ cm is compensated by a reduction in J_{OH} near $r = 0$. Consequently, $q(0)$ increases, which tends to stabilize the n=1, m=1 kink mode. The flatter total current profile near the q=2 surface may also stabilize the n=1, m=2 kink mode [13]. Conversely, a $J_{bd}(r)$ that is more peaked than $J_{OH}(r)$ has a destabilizing effect on the m=1 mode. The effect on the m=2 mode depends on the precise details of the beam deposition, density, and temperature profiles. (The effect of constant voltage operation is that q is reduced everywhere during co-injection, leading to reduced m=1 stability.)

In practice the effects of the beam-driven current on MHD stability and on the loop voltage may be complicated by changes in $T_e(r)$ and $Z_{eff}(r)$ during beam injection. It may be necessary to compute the plasma current density using measured profiles of plasma parameters to understand the detailed MHD effects of high power neutral-beam injection. The present results suggest that beam-driven currents can be a dominant factor in determining these effects.
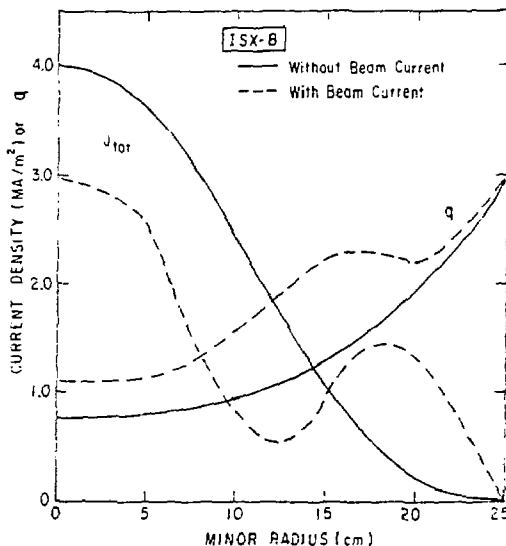
Fig. 3. Profiles of safety factor q and current density J_{tot} in ISX-B, at $<n_e> = 3.5 \times 10^{13}$ cm^{-3}, with ohmic heating alone (solid lines) and with beam-driven current (dashed lines). Total current is fixed at 0.20 MA.

REFERENCES

[1] Ohkawa, T., Nucl. Fusion 10 (1970) 185.

[2] Jassby, D. L., Nucl. Fusion 17 (1977) 309.

[3] Jassby, D. L., Proc. IAEA Conf. and Workshop on Fusion Reactor Design, Madison, Wisc., Oct. 10-21, 1977 (to be published).

[4] Connor, J. W., Cordey, J. G., Nucl. Fusion 14 (1974) 185.

[5] Cordey, J. G., Nucl. Fusion 16 (1976) 499.

[6] Jassby, D. L., Cohn, D. R., Parker, R. R., Nucl. Fusion 16 (1976) 1045.

[7] Equipe TFR, Nucl. Fusion 16 (1974) 279.

[8] Brusati, M., et al., Princeton Plasma Phys. Rep. PPPL-1403 (1977).

[9] Duchs, D. F., Post, D. E., Rutherford, P. H., Nucl. Fusion 17 (1977) 565.

[10] Corman, E. G., et al., Nucl. Fusion 15 (1975) 377.

[11] Lister, G. G., Post, D. E., and Rutherford, P. H., Plasma Heating in Toroidal Devices (Proc. 3rd Symp., Varenna, 1976) 303.

[12] PLT Group, in Plasma Physics and Controlled Nuclear Fusion Research (Proc. 7th Int. Conf., Innsbruck, Austria, 1978) to be published.

[13] Glasser, A.H., Furth. H. P. and Rutherford, P. H., Phys. Rev. Lett. 38 (1977) 234.